

DESY SR-78/06
May 1978

DESY-Bibliothek

7. JUNI 1978

UPS MEASUREMENTS OF CO CHEMISORBED AND CONDENSED ON RH(111)
USING SYNCHROTRON RADIATION

by

W. Braun and M. Neumann

*Fachbereich 4
Universität Osnabrück*

M. Iwan

II. Institut für Experimentalphysik der Universität Hamburg

E. E. Koch

Deutsches Elektronen-Synchrotron DESY, Hamburg

To be sure that your preprints are promptly included in the
HIGH ENERGY PHYSICS INDEX ,
send them to the following address (if possible by air mail) :

DESY
Bibliothek
Notkestrasse 85
2 Hamburg 52
Germany

UPS Measurements of CO Chemisorbed and Condensed on Rh(111)
Using Synchrotron Radiation

W. Braun and M. Neumann

Fachbereich 4, Universität Osnabrück, Albrechtstraße 28,
D - 4500 Osnabrück, FRG

M. Iwan

II. Institut für Experimentalphysik, Universität Hamburg,
Luruper Chaussee 149, D - 2000 Hamburg 50, FRG

and E.E. Koch

Deutsches Elektronensynchrotron DESY, Notkestieg 85,
D - 2000 Hamburg 52, FRG

Abstract

Photoemission data of the clean Rh(111) surface are strongly dependent upon photon energy in the range 15 eV to 27.5 eV. Three different chemisorption levels have been distinguished for CO chemisorbed on Rh(111) by exploiting the dependence of photoionization cross sections upon photon energy as well as of the orientation of the polarization of the electric field vector with respect to the molecular axis. Exciton-electron and electron-electron scattering dominates the intensity variations of the spectra of CO condensed on Rh(111). The origin of the observed energy level shifts of CO in the three different phases, gas, condensed and chemisorbed, are discussed in terms of relaxation, bonding and chemical shifts.

I. Introduction

Photoemission is a well established technique for the investigation of the electronic structure of clean metals and chemisorbed molecules. Recent reviews on this subject may be found in Ref. [1]. The correct assignment and the orientation of molecules on surfaces has become of particular interest recently [2-15]. The correct assignment for the symmetry of the molecular orbitals of chemisorbed species can be obtained by changing one of three parameters: (i) photon energy or (ii) polarization of the incident light and (iii) take off angle of the photoemitted electrons. Synchrotron radiation is a powerful tool for performing such experiments. It provides strongly polarized light as well as a wide and continuous photon energy range.

The photoelectron spectra of simple gases chemisorbed on surfaces are usually compared to the gas phase spectra (see e.g. Ref. 16). All these measurements show energy level shifts of the molecular orbitals in the chemisorbed phase with respect to the gas phase. Different mechanisms, such as relaxation-, chemical- and bonding shifts have been invoked for the origin of these shifts (see e.g. Ref. [6-19]). However, it is difficult to separate the main contributions to these shifts by comparing gas phase data to those of chemisorbed molecules only. More detailed information is expected by comparing the spectra of chemisorbed molecules with those of the gas phase as well as the solid. Such a comparison has been reported for hydro-

carbons on Ni(111) [17]. Here we present a comparison of CO chemisorbed and condensed on the Rh(111) surface.

The experimental set up is described in Section II. The photoelectron spectra of the clean Rh(111) surface and of CO chemisorbed and condensed onto it are given in section III. In section IV the photoelectron spectra of the clean Rh(111) surface are discussed in terms of the direct transition model. The photoemission data of CO chemisorbed on Rh(111) are discussed in terms of polarization dependent photoionization cross sections. Exciton-electron and electron-electron scattering dominates the intensity variations of the photoemission data of CO condensed on Rh(111). A comparison of the spectra of CO in three different phases yields information about the main contributions to the observed energy level shifts.

II. Experimental-Set up

Synchrotron radiation from the DESY SYNCHROTRON was used as a light source for performing the photoemission experiments. This enabled us to vary the photon energy continuously from 15 eV to 27.5 eV. The experimental equipment consisted essentially of a normal incidence monochromator [20] with 0.2 nm resolution and an UHV sample chamber with a base pressure in the low 10^{-10} mbar range. The angle of incidence of the p-polarized light was about 60° (Fig. 1a). The energy of the photoemitted electrons was analysed with

a Physical Electronics double-stage cylindrical mirror analyser. The axis of the analyser was normal to the incident light and lay in the plane of incidence. The half cone acceptance angle of the analyser was $42^\circ \pm 6^\circ$. Therefore the photoelectron spectra of single crystals contain usually information about selected symmetry lines in the Brillouin zone. Inherent with the analyser is a transmission function which overemphasizes the contribution from low kinetic energy electrons. The transmission follows fairly well a E^{-1} law. The joint resolution of the analyser and the monochromator was about 0.5 eV.

The sample consisted of a 0.6 nm thick slice with an area of $6 \times 8 \text{ mm}^2$. The (111) orientation was achieved via Laue back scattering. After spark cutting and mechanical polishing the sample was spot-welded between two tungsten wires which themselves were fixed via two copper rods to a rotatable liquid Helium flow cryostat. The temperature of the sample could be measured directly with a chromel-constantan thermocouple spot welded to the sample and indirectly via a Helium vapor pressure thermometer. The thermocouple allowed temperature measurements between 70 K and 1300 K. The vapor pressure thermometer measured the temperature at the bottom of the cryostat. This temperature was 5 K during the measurements. The temperature measured at this point was close to the temperature of the sample due to the excellent thermal contact.

Cleaning of the surface was achieved by direct heating the sample in 10^{-6} mbar oxygen at 1100 K. To restore the clean surface periodicity the sample was annealed at 1200 K for several hours in the residual gas. This cleaning procedure led to an atomically clean surface as has been proved in former LEED, Auger and SIMS experiments [21].

III. Results

A. Clean Rh(111) surface

For performing photoemission experiments it is important to select an appropriate experimental arrangement. The excitation process depends strongly upon the angle of incidence and, since we use synchrotron radiation as a light source, the polarization vector of the radiation. The direction of the photoemitted electrons is closely related to directions in the Brillouin zone. The cylindrical mirror analyser accepts electrons from a $42^\circ \pm 6^\circ$ cone with a tip of the cone at the illuminated spot of the sample (see Fig. 1a). In our experiment the axis of the cylindrical mirror analyser coincided approximately with the direction ΓW in the Brillouin zone (Fig. 1b). In the geometry applied in our experiment photoelectrons emitted from any point in the reduced Brillouin zone can be accepted with nearly the same probability by the analyser. Therefore photoelectron spectra measured in this geometry are largely averaged over steric angles. A different geometry, for example the cylindrical mirror analyser axis pointing in the $\Gamma - L$ (A) direction,

would overemphasize points along $\Gamma - U$, $\Gamma - W$ and $\Gamma - K$ (Σ) and neglect points of high symmetry along $\Gamma - X$ (Δ) and $\Gamma - L$ (Λ).

In Fig. 2 electron energy distribution curves for the clean Rh(111) surface are shown for photon energies ranging from 15 eV to 27.5 eV. The spectra shown in Fig. 2 have been obtained from the original data via the following normalization procedure. The measured spectra have been multiplied at each point by the corresponding kinetic energy of the photoelectrons in order to compensate for the analyser transmission function. Because the photon flux was not known the spectra have been adjusted in intensity relative to each other at points where no peaks due to the band structure of Rh were observed in the spectra. A different normalization procedure via the total photoelectric yield resulted in spectra with comparable relative peak heights.

Considerable amount of structure is observed in the photoelectron spectra down to 5.5 eV below the Fermi edge E_F . The relative intensities of the observed peaks vary strongly with photon energy suggesting different contributions to the photoemission due to direct transitions in this photon energy range. The XPS data of Smith et. al. [22] and Hüfner et. al. [23] cannot be compared directly to the spectra of Fig. 2 although the XPS data as well as the data shown here are consistent with band structure calculations of Christensen [24] and Smith [25]. The low photon

energy ($h\nu \approx 12$ eV) photoelectron spectra also show band-structure effects [26,27].

B. CO-Adsorption on Rh(111)

In Fig. 3 the photoelectron spectra obtained after CO chemisorption at room temperature corresponding to an exposure of 1.3×10^{-4} Pa sec are shown. This exposure was achieved by admitting CO for 10 sec at a pressure of 1.3×10^{-5} Pa. The measured data have been treated in the same manner as the spectra of the clean surface. The work function of the Rh/CO System has been determined to be 5.5 eV. Additional emission features are observed compared to the spectra from clean Rh(111) (Fig. 2). There is an asymmetric peak at around 8 eV binding energy with respect to the Fermi level. A second extra emission peak occurs at binding energies around 11.2 eV. Both peaks change their positions and intensities with photon energy. We note, that the asymmetric peak at lower binding energy has a larger halfwidth than the feature at higher binding energy. Furthermore the emission from the Rh d-bands is attenuated in a nonuniform manner.

C. CO-Condensation on Rh(111)

Photoelectron spectra obtained from CO condensed on the Rh(111) surface are presented in Fig. 4. After cooling below 20 K the sample was heated to 1200 K in order to remove those species of the residual gas which had been adsorbed

on the sample surface during cooling. After flashing the sample reached its final temperature ($T < 20$ K) within 5 minutes. CO gas was admitted to the sample chamber for 200 sec at a pressure of 1.35×10^{-4} Pa resulting in a CO exposure of 2.7×10^{-2} Pa sec. The resulting film thickness was estimated to be 15 nm. The photoelectron spectra obtained from the CO films thus prepared have been corrected for the analyser transmission function in the same way as the data from clean Rh(111).

A change of the workfunction to 5.1 eV was observed. Structure in the binding energy region from 0 to 4 eV in the photoelectron spectra of CO condensed on Rh(111) is attributed to photoemission from the Rh 4d bands. The three peaks in the region from 4 eV to 14 eV are ascribed to the corresponding molecular orbitals of gaseous CO (5σ , 1π , 4σ). The relative separations of these peaks vary slightly with photon energy. The emission strength from these levels is strongly attenuated if the kinetic energy of the photoelectrons exceeds 8 eV with respect to the vacuum level, because at these energies exciton electron scattering becomes possible. The arrows in Fig. 4 indicate the onset of this strong scattering mechanism.

IV. Discussion

A. Photoemission from the Clean Rh(111) Surface and Comparison to the Band Structure of Rh

The photoelectron spectra shown in Fig. 2 can be directly

interpreted using the band structure calculations of Christensen [24]. The results of this calculation are shown in Fig. 5. In this calculation the electron configuration of the isolated Rh atom ($4d^8 5s^1$) was used. On the basis of the RAPW-approximation [28] the eigenvalues corresponding to 9 bands at 89 points of the reduced Brillouin zone have been calculated. Figure 5 shows the band structure along lines of high symmetry (e.g. at 27 different points). The eigenvalues at points of lower symmetry are tabulated in Ref. [24]. Band 1 is derived from the atomic 5s level, bands 2 to 6 and 7 to 9 correspond to the atomic 4d and 5p levels, respectively. This band structure suggests that the density of initial states should peak at 1.1 eV, 2.3 eV, 2.8 eV and 5.3 eV below the Fermi level. The density of initial states calculated by Christensen [24] confirms this fact. Applying the direct model we expect peaks in the photoelectron spectra when for a given photon energy transitions between flat occupied to flat unoccupied energy bands are possible.

The high density of initial states at 1.1 eV originates from band 4 around the W point, bands 5 and 6 around Γ with large contributions from the Λ and Σ directions. At W transitions from band 4 to bands 7, 8 and 9 are allowed in the photon energy range 11 eV to 14 eV. A peak is observed in the measured spectrum at $\hbar\omega = 15$ eV (Fig. 2). This peak has changed to a shoulder at $\hbar\omega = 17.5$ eV and 20 eV which is consistent with the band structure calcula-

tion. Around Γ transitions from bands 5 and 6 become allowed to band 9 at 22.5 eV and at $\Lambda = (222)$ at 25 eV. A peak is observed at $\hbar\omega = 22.5$ eV. On the basis of this band structure calculation which omits the 4f levels the emission from the occupied d-bands is much stronger than expected at $\hbar\omega = 25$ eV and 27.5 eV. We expect that emission observed at higher photon energies is due to transitions from d-bands 5 and 6 along Λ to empty 4f bands. Transitions from band 5 and 6 to 7 and 8 along Λ are not observed in the spectra because the expected transition energies (18.5 eV to 19 eV) are between the chosen excitation energies (17.5 eV and 20 eV). In addition a peak at 1.7 eV binding energy excited with $\hbar\omega = 17.5$ eV is observed. This peak can be ascribed to transitions from band 4 to 8 in the Q direction. The peak at 2.3 eV below the Fermi level in the 15 eV spectrum corresponds to transitions from band 3 to 7, 8 and 9 around point (380). The high density of initial states at 2.8 eV in the theory of Christensen [24] is clearly seen in the 20 eV spectrum at 2.5 eV binding energy because at this photon energy transitions from the extremely flat bands 2, 3 and 4 along Λ are allowed to band 7 and 8. At lower photon energies this peak is not observed in accordance with theory. At a photon energy of 22.5 eV this peak has decreased due to increasing curvature in band 8. At the highest photon energies transitions to band 9 become allowed. The emission strength of these transitions is low compared to transitions to the f-like bands.

They are therefore observed only as shoulders in the spectra. The low energy peak in the $\hbar\omega = 17.5$ eV originates essentially from transitions from band 2 to 7 around the X point whereas transitions to band 8 and 9 are observed at $\hbar\omega = 20$ eV and 22.5 eV. The width of the occupied d-bands is $6.0 \text{ eV} \pm 0.5 \text{ eV}$ in good agreement with theoretical [24] (5.5 eV) and x-ray photoemission data (6 eV) [22,23].

B. Chemisorption of CO

In order to demonstrate the changes in the UPS spectra due to CO adsorption more clearly, the difference spectra shown in Fig. 6 have been derived from the data of Figs. 2 and 3. The most significant observations are: (i) the CO induced extra emission intensities and (ii) the shape of the reduction in the emission from the d-bands vary with photon energy. The energy dependence of the CO induced extra emission has been recently reported for CO chemisorbed on Ni [8,9], Cu [10], Ir [6,7] and Pd [5]. It has been explained as due to a resonance in the photoionization cross section by comparison with partial photoionization cross section measurements [29] and calculations [13,30] for CO in the gas phase. Both, the calculations and the measurements yield maxima in the photoionization cross section of the 4σ and 5σ levels. Theory predicts a maximum for the 4σ level at $\hbar\omega = 36$ eV, whereas this maximum is observed at $\hbar\omega = 32$ eV for CO in the gas phase and around $\hbar\omega = 36$ eV for CO chemisorbed on some of the transition metals. A similar behavior is observed for the 5σ level of CO. The

resonance in the photoionization cross section of this level occurs at 8 eV lower photon energies in the gas phase and 4 to 5 eV in the chemisorbed phase. The photoionization cross section of the 1π level decreases continuously with photon energy starting at $\hbar\omega = 20$ eV with an indication of a resonance close to the vacuum level. These resonances discussed occur at final state energies where the antibonding 2π and 6σ levels are expected.

The behavior of the photoionization cross sections can be understood on the basis of the dipole selection rules. The dipole transition matrix element $\langle f | \vec{A} \cdot \vec{\nabla} | i \rangle$ must be invariant under the symmetry operations of the CO molecule ($C_{\infty v}$). Applying the symmetry operations to the dipole matrix element the allowed transitions can be deduced for the electric field vector parallel (A_{\parallel}) or normal (A_{\perp}) to the molecular axis. In the dipole matrix element the total wave functions of the initial and final state have to be taken into account. For clarity the corresponding transitions are tabulated in Table I in a simple one electron picture. Keeping in mind that the 2π level is involved in the chemical bond of the chemisorption state the 2π level is expected to be split. The intensity of the allowed transitions is dependent upon the orientation of the CO molecule on the metal surface and the polarization vector of the incident light. In the present experiment the light was p-polarized. Incident and reflected light interact to produce

a standing wave field [11], an effect well known in infrared reflection absorption spectroscopy [31]. Therefore the electric field vector component normal to the surface is expected to be much stronger than the parallel component, especially in the chosen geometry. Recently evidence was found that CO is oriented normal with respect to the metal surface with carbon end down on Ni(100) [4,32], Ni(111) and Pt(111) [3]. Assuming the same orientation of CO on Rh(111) strong transitions from the 4σ and 5σ levels to the 6σ level and from the 1π level to the 2π level are expected for the electric field vector component normal to the surface (A_{\parallel} in Table I).

In accordance with this discussion, the energy dependence of the observed CO peaks (Fig. 6) can be explained. Emission from the 4σ level at a binding energy of 11.2 eV starts at $\hbar\omega = 22.5$ eV and increases with photon energy. As our measurements have been limited to photon energies below $\hbar\omega = 30$ eV the maximum in emission intensity could not be observed. The emission intensity from the more weakly bound CO levels ($1\pi + 5\sigma$) passes a minimum in the considered photon energy range. Inspection of the peak positions shows a difference in binding energy of about 0.5 eV at $\hbar\omega = 27.5$ eV and $\hbar\omega = 15$ eV respectively. The peak maximum, observed in the 27.5 eV spectrum at 8.3 eV binding energy is attributed to the 5σ level, whereas the shoulder is due to emission from the 1π level. Lowering the photon energy the emission

from the 5σ level decreases and the emission from the 1π level increases. The binding energy of the 1π level has been estimated to be 7.8 eV. Applying Davenport's theory [13] of the oriented free molecule to our experimental geometry the intensity ratios of the observed peaks in Fig. 6 are described reasonably well; e.g. the intensity ratio of the 5σ to the 4σ level is expected to be about 3:1 at $\hbar\omega = 28$ eV, emission from the 1π level is expected to be small at $\hbar\omega = 21$ eV and 28 eV when compared to the 5σ level. A comparison to CO in the gas phase concerning photoionization cross sections is difficult, because in the gas phase the molecules are arbitrarily oriented and contributions of A_{\perp} and A_{\parallel} are averaged. In contrast to the experimental data of Fig. 6 emission from the 1π level to the 6σ level is present in the gas phase spectra.

At a first glance the reduction in emission intensity in the d-band region due to CO chemisorption seems to be uniform, that is the attenuation would resemble the scaled negative photoelectron spectrum of the corresponding clean surface. Such a uniform attenuation can be explained by an additional scattering in the CO overlayer. It should be the same for a given kinetic energy of the photoelectrons. However, this is not borne out by our experiment. While the simple attenuation might be present, we consider a different dominating mechanism as recently suggested by Doyen [33]. He described the chemisorption state as a linear combination of molecular orbitals and metal d-states. In this

model Doyen [33] obtained an interference term for the transition amplitude resulting in large contributions to the difference emission from the d-bands. The emission can be enhanced or attenuated. Additional emission can also originate from the above mentioned split 2π level which may be partially occupied due to back donation [34]. Extra emission (eventually at 1.5 eV below E_F) cannot be clearly distinguished in the difference spectra. However, it is evident that the emission is most strongly reduced close to the Fermi Level. The states close to the Fermi level occupy bands 3 to 6 (see Fig. 5). Thus we suggest that these four bands are mainly involved in the chemisorption bond.

C. CO-Condensed on Rh(111)

In contrast to metals, electron-electron scattering and exciton-electron scattering become possible in insulators and semiconductors only if the kinetic energy of the excited electron exceeds a threshold energy. In the exciton-electron scattering process an excited electron is scattered to a lower lying state in the conduction band and a second electron is excited simultaneously to a localized state (e.g. a Frenkel exciton) within the band gap. This scattering mechanism becomes possible if the energy of the excited electron with respect to the bottom of the conduction band exceeds the excitation energy for a localized state. Thus exciton-electron scattering can occur only if

the excitation energy exceeds the sum of the band gap energy and the energy required to excite a localized state (see e.g. Ref. [35]). For electron-electron scattering an excitation energy of at least twice the band gap energy is necessary.

The threshold for exciton-electron scattering is clearly seen in the spectra of Fig. 4 and indicated by the arrows. The intensity of electrons with kinetic energies higher than 8 eV with respect to the vacuum level is strongly attenuated. Thus the apparent intensities of the CO-bands (Fig. 4) are strongly affected by exciton-electron and electron-electron scattering. The minimum energy to excite a Frenkel exciton within the band gap of solid CO is 7.9 eV as obtained from ultraviolet transmission [36] and electron energy loss measurements [37]. From (i) the excitation energy for an exciton, (ii) the threshold energy for the onset of strong scattering and (iii) the position of the top of the valence band we obtain for an estimate of the band gap in solid CO 11.0 ± 0.5 eV. Exciton-electron scattering can also influence the apparent peak position in the energy distribution curves, when its onset coincides with a CO emission band. This effect is observed e.g. in the spectrum taken with $\hbar\omega = 25$ eV where the 4σ level seems to be shifted to higher binding energies.

The peak positions of all three levels as well as their re-

lative separations vary with photon energy by up to ± 0.4 eV. This observation can be ascribed to a dispersion of the occupied bands derived from the 4σ , 1π and 5σ molecular orbitals. Dispersion of the valence bands of solid rare gases of up to 1 eV have been predicted [38]. A dispersion of 1.7 eV has been observed for solid Xe [39]. Unfortunately no band structure calculations of solid CO exist till now. Both, for the solid and the chemisorbed phase excitation of vibrational side bands in molecular crystals as recently described by Gadzuk et al. [43,44] may also be responsible for the width of the bands. These considerations may suggest band structure effects in the chemisorbed phase [40-42]. However, no evidence for such a behavior is observed (Fig. 3).

D. Comparison of the photoelectron spectra of CO in different phases

For a discussion of the observed level shifts we refer to Fig. 6 where the energy levels of gaseous, chemisorbed and solid CO are compared. The vacuum level was chosen as the zero of the binding energy scale. The energies of the 5σ , 1π and 4σ levels of gaseous CO (14 eV, 17 eV and 19.7 eV) have been taken from Ref. [29]. These energies are vertical binding energies. Adiabatic and vertical transition energies are nearly identical for the 4σ and 5σ level and differ by about 0.4 eV for the 1π level [45] (see Fig. 7).

The one electron transition 5σ to 2π corresponding to the so-called "fourth positive band" $X^1\Sigma^+ + A^1\Pi$ is indicated for the gas by an arrow. The average peak positions of the 4σ , 1π and 5σ derived energy bands of solid CO as well as the energy of the exciton (Ex) [36] are given in the second column of Fig. 7. The Fermi level (E_F) and the bottom of the conduction band (BCB) as determined in the previous paragraph are also included. The energetic positions of the occupied levels of CO chemisorbed on Rh(111) are depicted together with the Fermi level (E_F) in the third column of Fig. 7.

Compared to the gas phase large level shifts in the different phases on Rh(111) occur. These shifts are due to initial as well as final state effects in the photoexcitation process [16-19,46]. The initial state is influenced by changes in the chemical environment and by the fact that chemical bonds may be formed. In particular bonds of certain molecular orbitals of adsorbed molecules and the substrate have to be considered. Shifts due to these effects are called chemical and bonding shifts, respectively. The bonding shift always yields larger binding energies. Differences in relaxation energies in different phases lead to final state shifts. The difference in relaxation energy originates from the dielectric screening of the positive hole created in the photoionization process and possibly from image-charge screening of the final state.

The latter is expected to be negligible in the insulating solid. The former will be denoted as polarization shift in the following discussion. Final state shifts are usually positive when gas phase spectra are compared to those of the solid or chemisorbed phase. Experimentally it is not possible to separate the level shifts unambiguously. However, theoretical considerations [19] and experimental data from different phases can yield an estimate of the main contributions.

A reduction in binding energy of the molecular orbitals up to 1.7 eV with respect to the gas phase has been observed in solid nitrogen and oxygen [47] and solid hydrocarbons [17]. This observation has been attributed to polarization. The difference in binding energy between gaseous and solid CO are 2.9 eV, 3.6 eV and 2.7 eV for the 5σ , 1π and 4σ level (Fig. 7). For CO chemisorbed on Rh(111) the 5σ level is observed at higher binding energy (-2.7 eV) compared to the solid whereas the 4σ level is shifted slightly to lower binding energies by + 0.3 eV. The 1π level does not change its position. The 5σ level is found to lie below the 1π level as for CO on Ni(100) [8] and Ir(111) [7] in contrast to CO on Cu(100) [10]. In the "van der Waals solid" CO a chemical shift does not exist. Therefore, the level shifts have to be attributed to differences in relaxation energy (polarization). For the different orbitals these shifts are not necessarily identical [16]. For

CO chemisorbed on Rh(111) possible chemical shifts have to be considered. A chemical shift of about -1.1 eV has been calculated for NiCO and Ni₂CO clusters for the levels not involved in the Ni-CO bond [19]. Similar calculations are not yet available for Rh-CO clusters. It is reasonable to assume chemical shifts of the same order of magnitude for CO chemisorbed on Rh(111). This suggests that the polarization energy is even larger (about 1 eV) in the chemisorbed phase. This larger value is still in accordance with theoretically predicted polarization energies of up to 4 eV [48]. A shift of 2.7 eV is observed for the 5 σ level when comparing CO chemisorbed and condensed on Rh(111). As the 5 σ molecular orbital forms the strong chemisorption bond with the metal d-orbitals the shift of 2.7 eV is attributed to the bonding shift. The bonding shift may be as large as 3.7 eV if we take into account that the polarization energy can be up to 1 eV larger than in solid CO. This value seems to be reasonable on the basis of the calculations of Bagus and Hermann who calculated bonding shifts of -3.3 eV and -3.4 eV for NiCO and Ni₂CO, respectively [18,19].

Finally we want to comment on the ordering of CO chemisorbed on Rh(111), Ni(100), Ir (111) and Cu(100). For Cu the heat of adsorption is 60 kJ/Mol [49], much lower than for CO on Ir(111) [50], Ni(100) [51] and Rh(111) [21,52] where about 130 kJ/Mol have been observed. The

lower adsorption energy is due to the weaker interaction of CO with the Cu(100) surface which results in a lower bonding shift. Therefore the 5 σ level lies slightly above the 1 π level for CO on Cu(100) [10].

V. Conclusions

The importance of comparing $\hbar\omega$ -dependent spectra from chemisorbed CO to both the gas phase and the solid phase spectra has become evident. Further a thorough understanding of the electronic properties of the clean surface is important for the interpretation of chemisorption data. The photoemission data of the Rh(111) surface could be explained in terms of Christensen's band structure calculations [24] in the direct transition model. Exploiting the dependence of photoionization cross sections upon photon energy as well as of the orientation of the polarization of the electric field vector with respect to the molecular axis three different chemisorption levels have been distinguished for CO chemisorbed on Rh(111). For p-polarized light a reduction of emission intensity for three of the six allowed transitions is obtained for molecules oriented normal to the surface because of the standing wave field effect.

For solid CO it was found that the variation of the inten-

sities of the observed peaks is strongly influenced by exciton-electron and electron-electron scattering. The onset of this scattering mechanism together with the excitation energy of a Frenkel exciton the band gap was deduced. The origin of the observed energy level shifts has been discussed. In particular, we have estimated shifts due to polarization and bonding of CO chemisorbed and condensed on Rh(111). Dispersion of energy bands, change in Franck-Condon factors, phonon side bands as well as the orientation of the molecules have to be considered in a thorough interpretation of photoemission data in the valence band region of condensed and chemisorbed molecules.

References

- [1] "Photoemission from Surfaces", ed. by B. Feuerbacher, B. Fitton and R. Willis, John Wiley and Sons, New York, 1977, and
B. Feuerbacher and B. Fitton, in "Electron Spectroscopy for Surface Analysis", ed. by H. Ibach, Springer Verlag, Heidelberg, New York, 1977, p. 151
- [2] J.C. Fuggle, M. Steinkilberg and D. Menzel, Chem. Phys. 11, 307 (1975)
- [3] G. Apai, P.S. Wehner, R.S. Williams, J. Stöhr and D.A. Shirley, Phys. Rev. Lett. 37, 1497 (1976)
- [4] R.J. Smith, J. Anderson and C.J. Lapeyre, Phys. Rev. Lett. 37, 1081 (1976)
- [5] T. Gustafsson, E.W. Plummer, D.E. Eastman and J.L. Freeouf, Solid State Commun. 17, 391 (1975)
- [6] G. Brodén, T.N. Rhodin, C. Brucker, R. Benbow and Z. Hurych, Surface Sci. 59, 593 (1976)
- [7] T.N. Rhodin and C. Brucker, in Proc. 7th Intern. Vac. Congr. and 3rd Intern. Conf. Solid Surfaces (Vienna 1977) p. 371
- [8] C.L. Allyn, T. Gustafsson and E.W. Plummer, Chem. Phys. Lett. 47, 127 (1977)
- [9] C.L. Allyn, in Proc. 7th Intern. Vac. Congr. and 3rd Intern. Conf. Solid Surfaces (Vienna 1977) p. 497
- [10] C.L. Allyn, T. Gustafsson and E.W. Plummer, to be published

- [11] E.W. Plummer, in Proc. 7th Intern. Vac. Congr. and 3rd Intern. Conf. Solid Surfaces (Vienna 1977) p. 647
S.P. Weeks and E.W. Plummer, Solid State Commun. 21, 695 (1977)
- [12] P.M. Williams, P. Butcher, J. Wood and K. Jacobi, Phys. Rev. B14, 3215 (1976)
- [13] J.W. Davenport, Thesis, University of Pennsylvania (1976), unpublished
- [14] I.P. Batra and P.S. Bagus, Solid State Commun. 16, 1097 (1975)
- [15] W. Heiland, W. Englert and E. Taylauer, Am. Vac. Soc. Meeting, Boston, Mass. USA, November 1977
- [16] C.R. Brundle, in "Proceedings of the NATO Advanced Study Institute on Electronic Structure and Reactivity on Metal Surfaces", ed. by E.G. Derouane and A.A. Lucas, Plenum Press, New York, 1976, p. 389
- [17] J.E. Demuth and D.E. Eastman, Phys. Rev. Lett. 32, 1123 (1974)
- [18] P.S. Bagus and K. Hermann, Solid State Commun. 20, 5 (1976)
- [19] K. Hermann and P.S. Bagus, Phys. Rev. B16, 4195 (1977)
- [20] N. Schwentner, A. Harmsen, E.E. Koch, V. Saile and M. Skibowski, in "Vacuum Ultraviolet Radiation Physics", ed. by E.E. Koch, R. Haensel and C. Kunz, Pergamon-Vieweg, Braunschweig, 1974, p. 792

- [21] W. Braun, M. Neumann and G. Meyer-Ehmsen, to be published
- [22] N.V. Smith, G.K. Wertheim, S. Hüfner and M.M. Traum, Phys. Rev. B10, 3197 (1974)
- [23] S. Hüfner, G.K. Wertheim and D.N.E. Buchanan, Solid State Commun. 14, 1173 (1974)
- [24] N.E. Christensen, phys. stat. sol. (b) 55, 117 (1973)
- [25] N.V. Smith, Phys. Rev. B9, 1365 (1974)
- [26] M.M. Traum and N.V. Smith, Phys. Rev. B9, 1353 (1974)
- [27] D.T. Pierce and W.E. Spicer, Phys. Rev. B5, 2125 (1972)
- [28] N.E. Christensen and B.O. Seraphin, Phys. Rev. B4, 3321 (1971)
- [29] E.W. Plummer, T. Gustafsson, W. Gudat and D.E. Eastman, Phys. Rev. A15, 2339 (1977)
- [30] J.W. Davenport, Phys. Rev. Lett. 16, 945 (1976)
- [31] R.G. Greenler, J. Chem. Phys. 44, 310 (1965)
- [32] K. Horn, A.M. Bradshaw and K. Jacobi, Surface Sci., in press
- [33] G. Doyen and G. Ertl, in Proc. 7th Intern. Vac. Congr. and 3rd Intern. Conf. Solid Surfaces (Vienna 1977), p. 703
- [34] G. Blyholder, J. Phys. Chem. 68, 2772 (1964)

- [35] N. Schwentner, Phys. Rev. B14, 5490 (1976)
- [36] S.R. Scharber, Jr. and S.E. Webber, J. Chem. Phys. 55, 3977 (1971)
- [37] H.J. Hinz, in Proc. IVth Intern. Conf. Vacuum Ultra-violet Radiation Physics, Pergamon/Vieweg, Braunschweig, 1974, p. 176, and U.D. Meyer, A. Skerbele and E.N. Lassetre, J. Chem. Phys. 43, 805 (1965)
- [38] U. Rössler, phys. stat. sol. 42, 345 (1970), *ibid* (b) 45, 483 (1971)
- [39] N. Schwentner, P.-J. Himpfel, V. Salle, M. Skibowski, W. Steinmann and E.E. Koch, Phys. Rev. Lett. 34, 528 (1975)
- [40] R.V. Kasowski, Phys. Rev. Lett. 37, 219 (1976)
- [41] R.V. Kasowski, Surface Sci. 63, 370 (1977)
- [42] K. Horn, A.M. Bradshaw and K. Jacobi, J. Vac. Sci. Techn., in press
- [43] J.W. Gadzuk, Phys. Rev. B14, 5458 (1976)
- [44] P.R. Norton, R.L. Tapping, H.P. Broida, J.W. Gadzuk and B.J. Waclawski, Chem. Phys. Lett. 53, 465 (1978)
- [45] D.W. Turner, C. Baker, A.D. Baker and C.R. Brundle, "Molecular Photoelectron Spectroscopy", Wiley-Interscience, London, 1970

- [46] T. Gustafsson and W.E. Plummer, in "Photoemission from Surfaces", ed. by B. Feuerbacher, B. Fitton and R. Willis, John Wiley and Sons, New York, 1977, p. 753
- [47] F.-J. Himpfel, N. Schwentner and E.E. Koch, phys. stat. sol. (b) 71, 615 (1975)
- [48] E.W. Plummer, in "The Physical Basis for Heterogeneous Catalysis", ed. by E. Drauglis and R.I. Jaffee, Plenum Press, New York, 1975, p. 203
- [49] J.C. Tracy, J. Chem. Phys. 56, 2748 (1972)
- [50] J. Küppers and A. Plügge, J. Vac. Sci. Technol. 13, 259 (1976), and C.M. Comrie and W.H. Weinberg, J. Chem. Phys. 64, 250 (1976)
- [51] J.C. Tracy, J. Chem. Phys. 56, 2736 (1972)
- [52] D.G. Castner, B.A. Sexton and G.A. Somorjai, Surface Sci. 71, 519 (1978)

Table I: Allowed transitions for the electric field vector parallel ($A_{||}$) or perpendicular (A_{\perp}) to the molecular axis of CO.

Electric Field Vector	$A_{ }$	A_{\perp}
Allowed Transitions	4 σ + 6 σ	1 π + 6 σ
	5 σ + 6 σ	
	1 π + 2 π	4 σ + 2 π 5 σ + 2 π

Figure Captions:

Fig. 1a: Experimental geometry used for our synchrotron-radiation measurements. \hat{n} is a unit vector along the surface normal. \vec{E} is the electric field vector.

Fig. 1b: Brillouinzone of an fcc lattice

Fig. 2: Photoelectron energy distributions for the clean Rh(111) surface obtained with different photon energies (p-polarization). The spectra, plotted with respect to the Fermi level, are displaced to each other proportional to the photon energies used.

Fig. 3: Photoelectron energy distributions for CO chemisorbed on the Rh(111) surface obtained with different photon energies (p-polarization). The spectra, plotted with respect to the Fermi level, are displaced to each other proportional to the photon energies used.

Fig. 4: Photoelectron energy distributions for CO condensed on the Rh(111) surface obtained with different photon energies (p-polarization). The spectra, plotted with respect to the Fermi level, are displaced to each other proportional to the photon energies used.

ton energies used. The arrows indicate the onset of electron-exciton scattering. The shaded area of the uppermost curve indicates the contributions of the unscattered electrons from the condensed overlayer.

Fig. 5: RAPW bandstructure of Rhodium reproduced from Ref. [24] (with permission).

Fig. 6: Difference spectra of CO chemisorbed on Rh(111)

Fig. 7: Energy level diagram of CO in different phases. For all levels vertical energies are given. The vacuum level is chosen as reference level. BCB is the bottom of the conduction band. Ex is the energetic position of a Frenkel exciton with the lowest excitation energy.

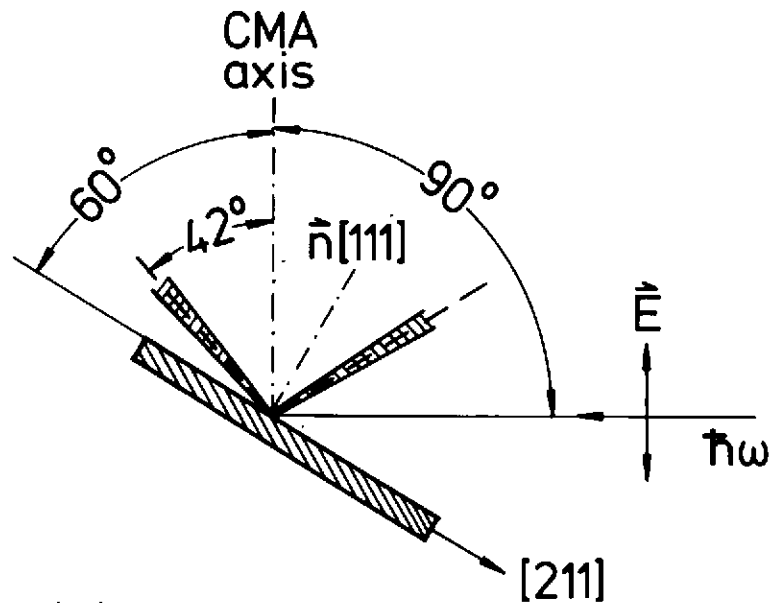


Fig. 1a

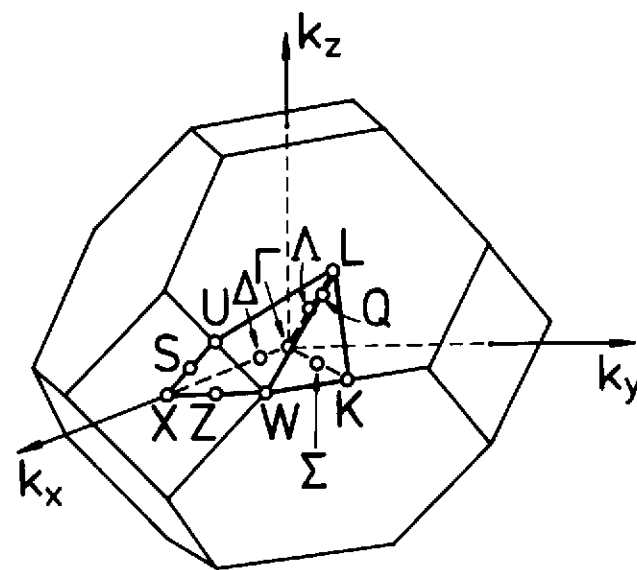


Fig. 1b

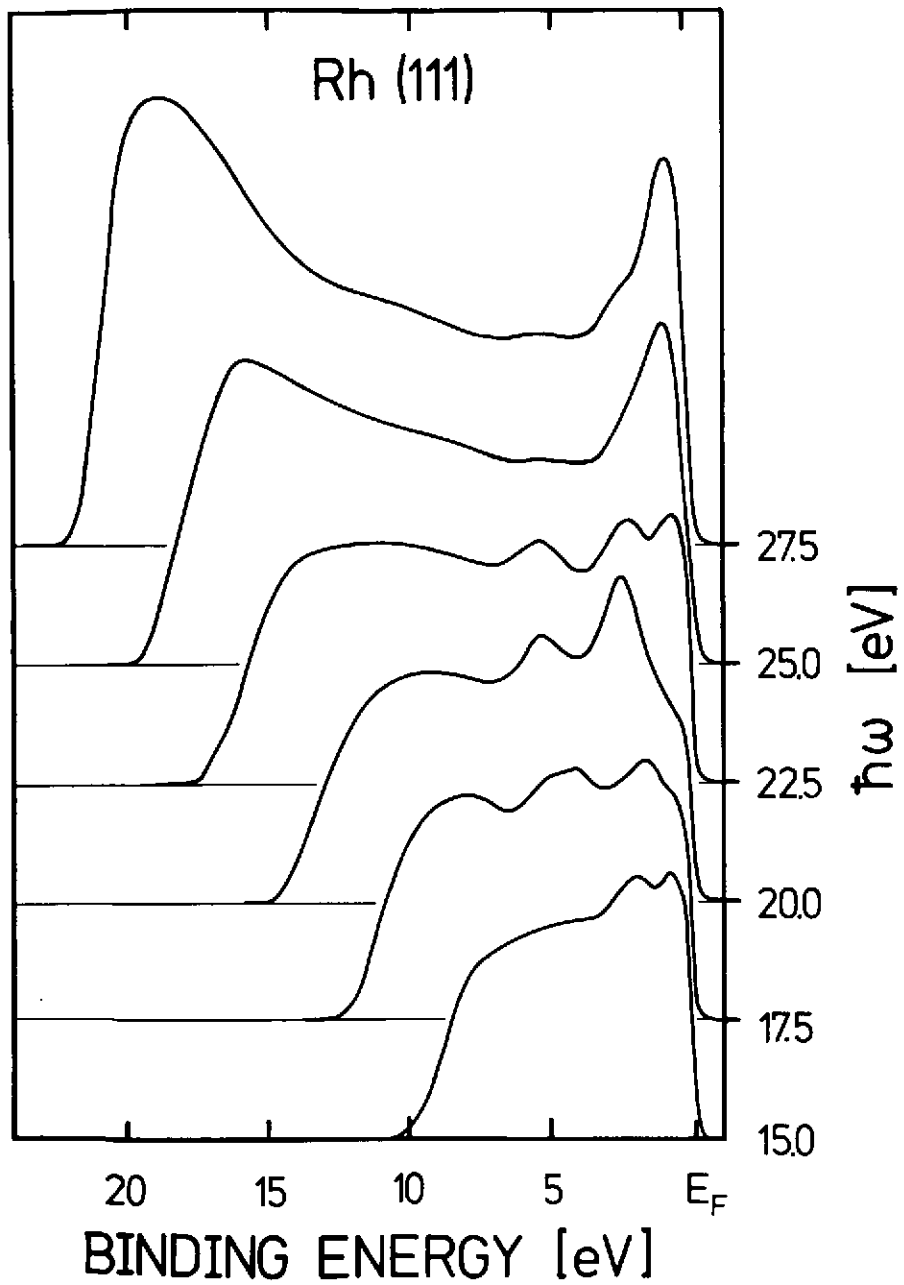


Fig. 2

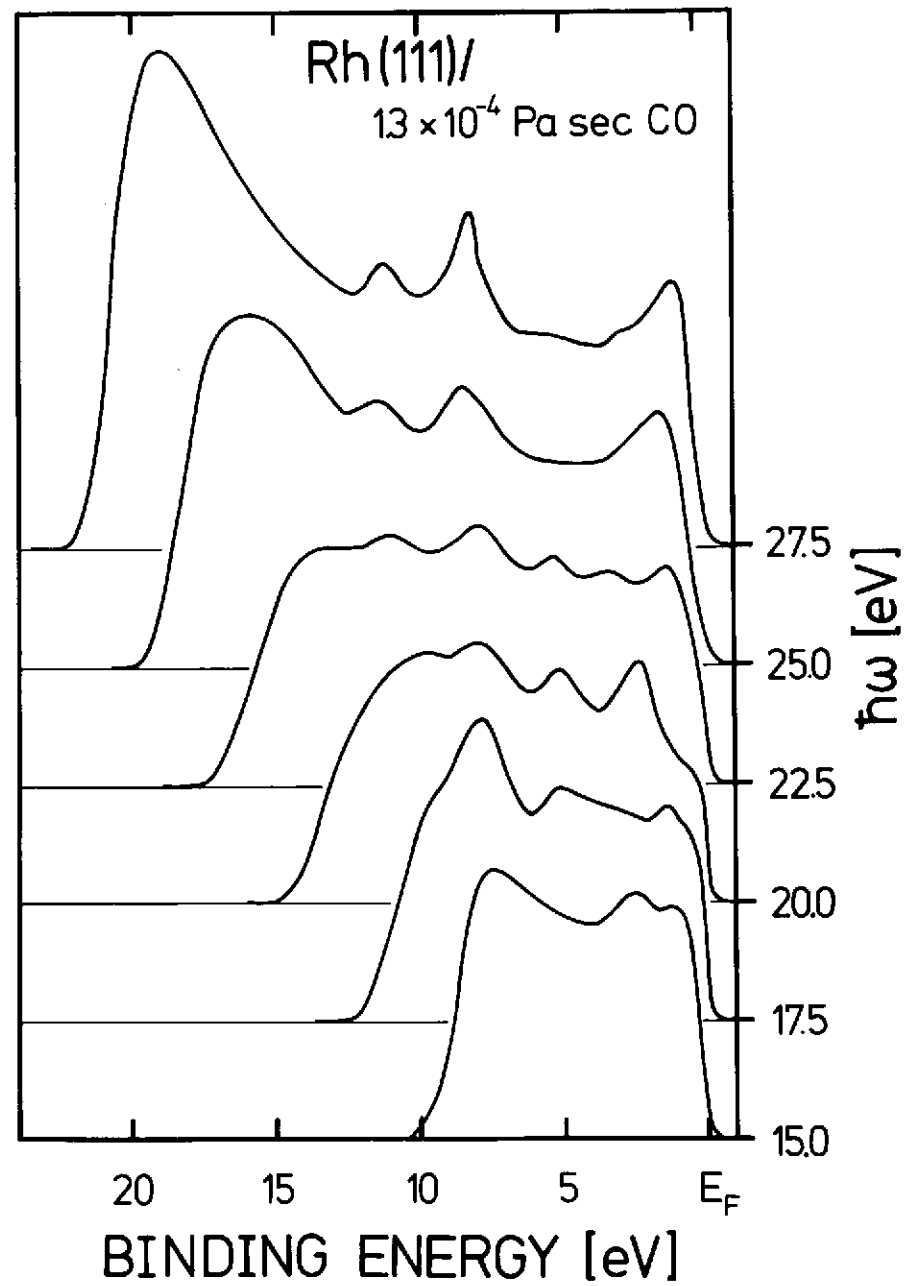


Fig. 3

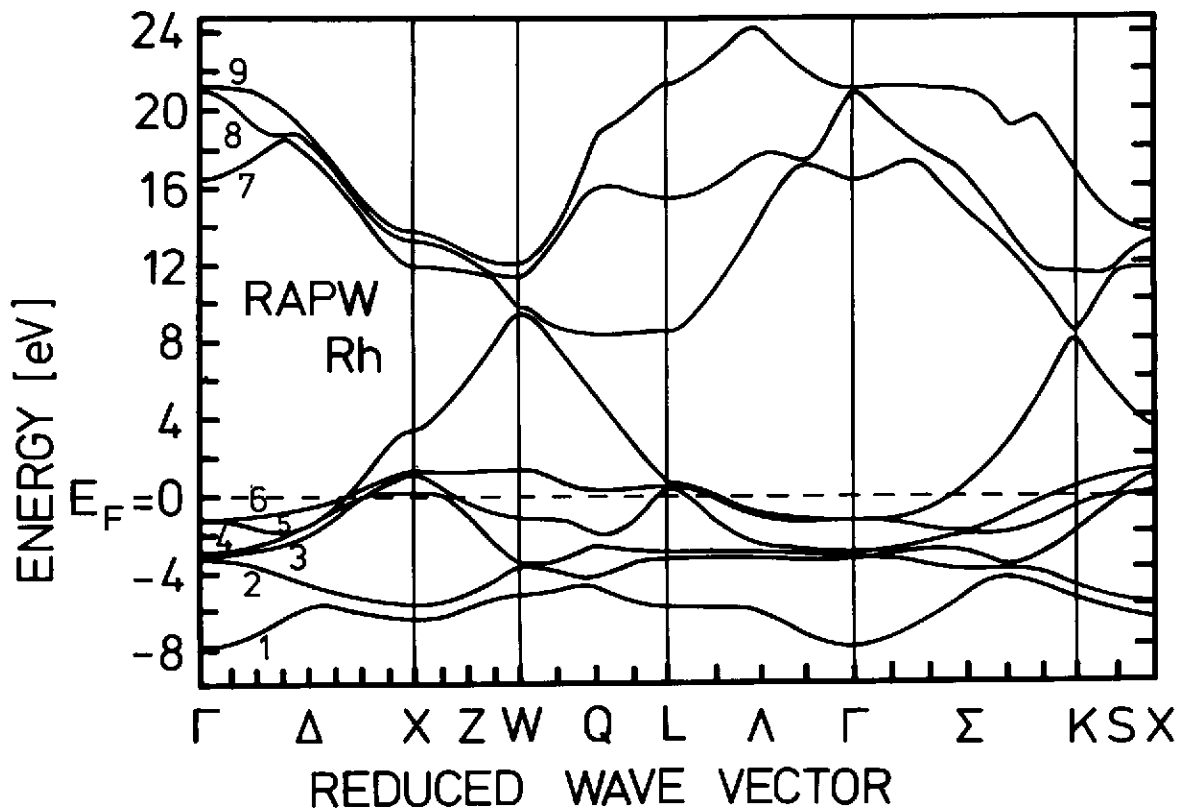


Fig. 5

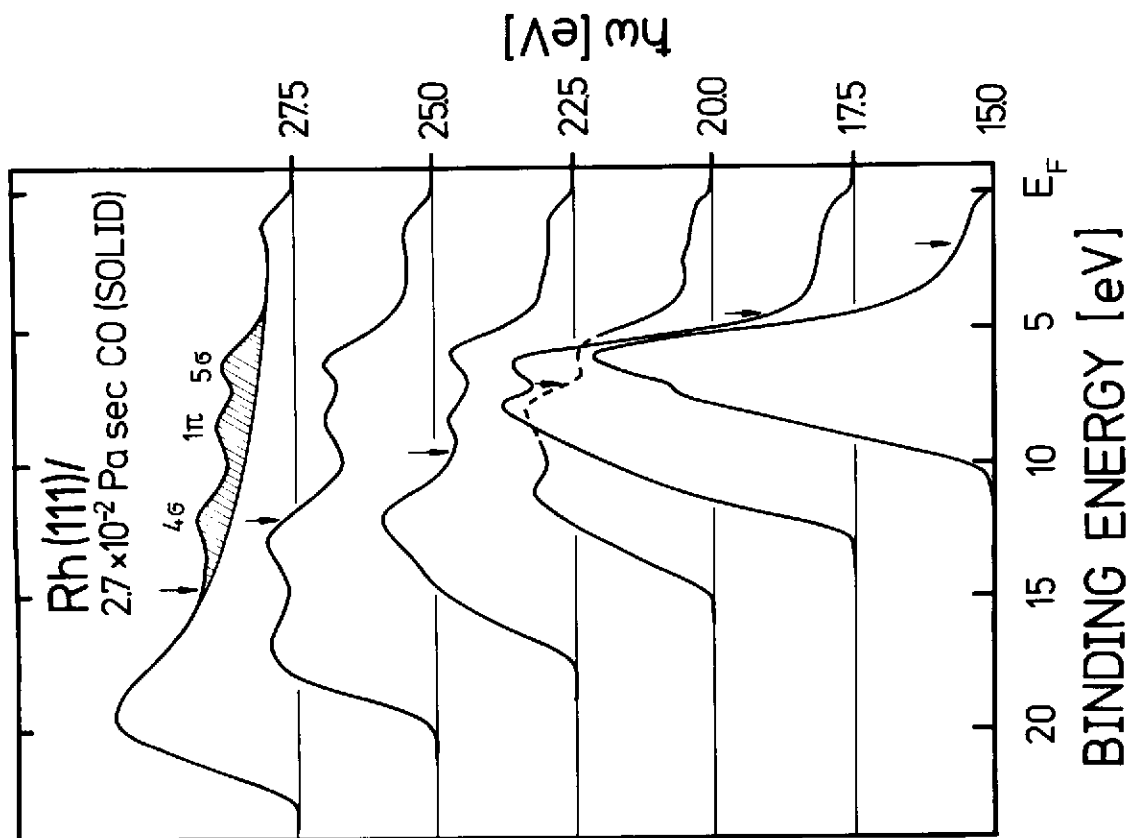


Fig. 4

